Multi-Pressure Rail System Design with Variable Pressure Control Strategy

Xiaofan Guo*, Riccardo Madau*, Jacob Lengacher*, Andrea Vacca*, and Rafael Cardoso**

Purdue University, Maha Fluid Power Research Center, 1500 Kepner Drive, Lafayette, IN, USA*
Bosch Rexroth Corporation, 8 Southchase Court, Fountain Inn, SC, USA**
E-Mail: guo92@purdue.edu

This paper presents the design and the control method of a Multiple Pressure Rail system (MPR) with a variable pressure control logic that allows minimization of throttling loss, therefore, increasing the overall fluid power actuation efficiency. An MPR system allows controlling hydraulic actuators with a pressure control logic, as opposed to traditional flow control logics which are well established in mobile applications. A proper setting of the number of pressure rails and the pressure level in each rail permits optimizing the system efficiency of an MPR solution. MPR systems have been recently proposed with different purposes, but seldom adopt variable pressure control strategies to manage the pressure variations in the rails. Moreover, the related past work attempts to maximize the energy recovery during overrunning load conditions. This paper, instead, addresses the case of an MPR system that handles a multitude of hydraulic functions without significant overrunning loads, as it occurs in many mobile applications such as in agriculture. The paper first presents the design alternatives considered for the MPR system, including the supply, the control valves, and the controller. Second, a dedicated test rig is developed to support experimental activities and validations of a lumped parameter model developed within this research to develop the MPR control strategy. The results describe the operating features of the proposed MPR solution. By considering the case of a traditional LS system, the paper results also show how system efficiency can be highly improved, with energy savings in the order of 49%.

Keywords: System Efficiency, System Design, Control, Experiment
Target audience: Agricultural Machinery, Mobile Hydraulics, Mining Industry

1 Introduction

Fluid power systems for off-road mobile applications typically adopt centralized architectures, such as the load sensing system (LS) or open center systems. In these architectures, each working line's flow is controlled according to the instantaneous actuator request, and throttling losses are always present in cases of an imbalance in the load between actuators [1]. The energy transmission efficiency of such systems can reach values much higher than the 21% average found in mobile applications [2]. Significant is the case of an agricultural tractor investigated by the authors' team, where efficiency values for the circuit supplying the hydraulic remotes were found to be up to 56% [3]. However, off-road machines using hydraulic remotes, such as tractors, often utilize each hydraulic remote connection to supply multiple actuators with dedicated flow control valves. In such condition, the LS remote valve is set to maximum opening, to ensure to fulfil the request of the downstream flow control valves installed in the implement. This causes the supply pump to not follow the flow command established by the remote valve, so that the pump enters into a pressure saturation condition determined by the absolute pressure limiter of the pump. In this circumstance, the supply pressure usually largely exceeds the pressure established by the actuators at the implement. Consequently, the power loss due to throttling becomes excessive, and bringing the overall system efficiency to values typically below 20%. Therefore, there is a need for higher energy efficiency hydraulic architectures that are suitable to power hydraulic remotes with numerous actuators.

The literature presents several studies to improve the efficiency of a LS system. A significant example is the work by Tian et al. [4], which proposed a hybrid variable margin method to adjust the pump pressure and reduce the

throttling loss occurring at the LS valve. This method, however, does not address the problem of inefficiency due to load imbalance. Siebert et al. [5] proposed a method that elevates the load pressure of the low load actuators by connecting their outlet to a pressurized line with an accumulator. This method shows up to 44% decrease in the throttling loss in simulation. However, this method is penalized by a high load imbalance. Critically, the past work that improves the energy efficiency of LS system does not address the problem of having multiple actuators controlled by additional flow control valves downstream from the LS valve. Therefore, a different actuation control method is required. Among other methods specifically addressing energy efficiency, the displacement control method is probably the most attractive [6]. The displacement control strategy eliminates the need for flow throttling valves by directly setting the pump displacement to control the actuator. However, in principle, this method requires one supply unit per actuator, which is impractical for most off-road vehicles. Possible solutions for this problem were proposed; an example is the sharing control method [7]. Still, such a method is not suitable for systems that control actuators through hydraulic remotes, such as in a tractor-implement system.

A great potential alternative to the established flow control concepts is pressure control. The basic system that implements this kind of control is the constant pressure (CP) system. In a CP system the supply unit provides flow to a pressure rail to which all the actuators are connected via hydraulic control valves (often servo valves) [8]. There are many advantages associated with the CP system. For example, in the CP system, the supply unit and the actuators are decoupled, which enables the implementation of power management strategies for the prime mover. This separation can also enlarge the actuator control bandwidth since the actuator response is not affected by the dynamics of the supply unit. On the other hand, similarly to the LS solution that is well established in off-road vehicles, the efficiency of a traditional CP system is limited by the large throttling losses between the supplying rail and the actuators with lower loads.

To address the above issue, advanced CP systems have been recently formulated [9]. Such systems keep the advantages from the basic CP system while improving the system efficiency. These advanced CP systems can be grouped into two categories: secondary controlled-based and hydraulic transformer-based. Firstly, the secondary control concept [10] is a throttle-less actuation method originally formulated for hydrostatic transmissions which directly acts on the actuator to control its output (velocity or torque). An example in off-road application outside propulsion was given by Volvo [11], and proposed a novel variable area cylinder for a secondary controlled system and demonstrated 34-50% fuel efficiency improvement in a 30-ton excavator. Secondly, the hydraulic transformer is a device able to lower the pressure level from the constant pressure supply to the actuator level, without wasting power through throttling. The most significant designs are listed in [12], [13]. However, hydraulic transformers have not reached commercial success yet due to their complexity, reliability concerns, and high cost.

The multi-pressure rail (MPR) system is a promising expansion on the advanced CP systems, but does not strictly fit in either of the categories above. Lumkes et al. in [14] proposed a generic design of an MPR system with the goal of increasing system efficiency, control flexibility and system redundancy. In this work, the system was tested on a backhoe test rig, showing good functionality, though the efficiency was not specifically addressed and a controller design suitable for such a system was not proposed. Dengler et al. in [15] and [16] proposed a constant pressure system with intermediate pressure line. With the added intermediate pressure line, 20% efficiency improvement are predicted through theoretical calculation compared to a standard LS system. The most relevant past effort is represented by the STEAM excavator by RWTH Aachen [17] [18], and the hybrid hydraulic-electric architecture (HHEA) [19]. Both systems used pressure rail technology. The STEAM machine experimentally demonstrated up to a 30% reduction in fuel consumption. This improvement was achieved thanks to the energy recovery occurring during overrunning load conditions, and by the relatively short actuation period of each function, suitable to accommodate engine management strategies. HHEA system took the concept one step further by adding a hydraulic motor with an electric machine to each actuator that replaced the traditional metering valve to reduce throttling loss. In the simulation study, HHEA system outperformed the STEAM system in energy consumption reduction by 40%, thanks to the throttle-less design. One important observation is that the above works on advanced CP systems targeted construction machinery, an application that involves a dynamic working cycle with many instances of overrunning load. Due to the complexity of the working cycle, the pressure in the rails was set to be constant without reducing the control effort. Opgenoorth et al. in [20] proposed an MPR system

for an electrified excavator with optimized rail pressure controller that shows a 29% efficiency improvement in simulation. However, also this work relates to mobile construction applications; moreover, no experimental validation for the design and control approach was provided.

This paper instead focuses on MPR systems with variable pressure logic conceived for reducing the throttling losses. The focus of this paper is not to address the case of machines with overrunning loads but is instead particularly convenient for replacing current systems for off-road vehicles with remote connections using multiple motor actuators, such as the agricultural applications mentioned above. Typically, the duty cycle for remote attachments, such as hydraulic implements (such as planters, baylers, seeders), present slow dynamics and very seldom instances of overrunning load conditions. Such implements also typically use primarily hydraulic motors running in one direction for actuators, and as such this paper analysis will focus primarily on motor-only applications.

Figure 1 shows a generic MPR system as considered in this work. It includes a supply system, pressure rails, pressure selection and control valves, and actuators. The pressure selection and control valve pick the best combination of inlet and outlet pressure from the rails to the actuator based on the actuator load pressure to minimize the throttling loss through the valves.

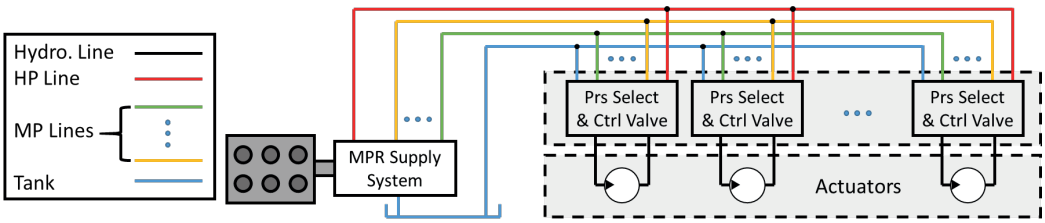

Figure 1: Generic MPR System Design.

The working principle for a three rail MPR system is schematically shown in **Figure 2** (there-rail MPR). For a hydraulic motor, the different combinations of inlet and outlet pressure create different theoretical output torque (shown as the dashed horizontal lines on the figure). As the flow rate Q_L increases, the pressure loss across the control valves becomes significant, varying the output torque for the same pressure difference. The curved solid lines correspond to the adjusted torque when accounting for the valve pressure losses. If the controlled actuator has a resistive torque, as in point T_1, then the control system will select a torque setting just above T_1, represented by the red line. The on/off valve set connects the motor inlet to the medium pressure-rail and the motor outlet to the low-pressure rail, while the metering valves control the speed of the actuator. For an overrunning load T_2, the system instead selects a torque setting right below the actuator load.

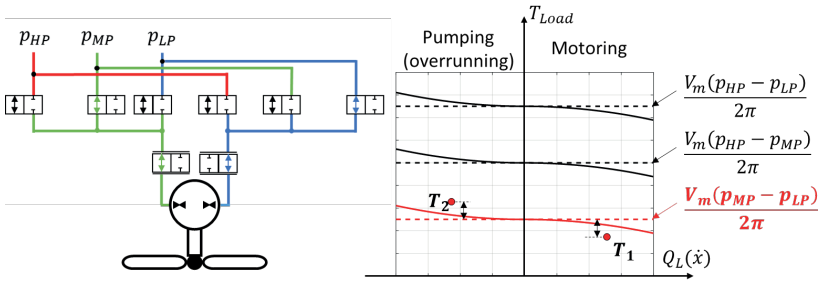

Figure 2: Working Principle for MPR System for motor actuator.

In summary, this paper develops and demonstrates a new design and control method for a MPR system that fits the case of off-road vehicles requiring centralized architectures and multiple motor actuators. Such a system is appropriate for applications such as agricultural tractors and their implements. The system improves energy efficiency by limiting the throttling losses. This paper first describes the conceptual design of the MPR system in section 2, considering different implementation variants for the two main subsystems: the hydraulic supply and the pressure selection and control valves. Then, section 3 describes the controller used to regulate the actuator speeds and to determine the pressure levels. In section 4, the paper describes the design of the MPR test rig that is

used to validate the control strategies. Section 5 then presents presents the results collected from the test rig, using them to validate a simulation and generate estimated efficiency gains for the proposed system.

2 MPR System Design

The MPR system is divided into four parts (Figure 1): pressure rails, supply system, pressure selection and control valve set, and actuators.

2.1 Number of Rail Selection

The number of rails determines the number of different working pressure ranges for the system, referred to as modes in this study. The total number of possible modes for a given number of rails is calculated by Equation (1):

$$\#mode = \#rail^2 \tag{1}$$

Take a three-rail system as an example, the total number of possible modes is nine. However, not all those modes are necessary. As this work focuses on the monodirectional hydraulic motor as actuators, several modes can be eliminated. Modes such as HP-HP, MP-MP, LP-LP that connect the same pressure level to both inlet and outlet will not power a hydraulic motor at all. Where the mode is defined here by inlet rail – outlet rail. Moreover, as most of the hydraulic motors in agricultural applications are monodirectional, operating at fairly constant speed, with no significant overrunning loads, modes LP-HP, MP-HP, LP-MP are not needed. As a result, the relationship between the number of rails and the number of modes is modified as stated in Equation (2).

$$\#mode = \frac{\#rail(\#rail - 1)}{2} \tag{2}$$

As shown in **Figure 3**, more rails in the system allow for more modes for the actuators to choose from, and less throttling loss. Throttling loss could be eliminated entirely if the number of rails matched the number of actuators. However, the system cost control complexity increase greatly with the number of rails.

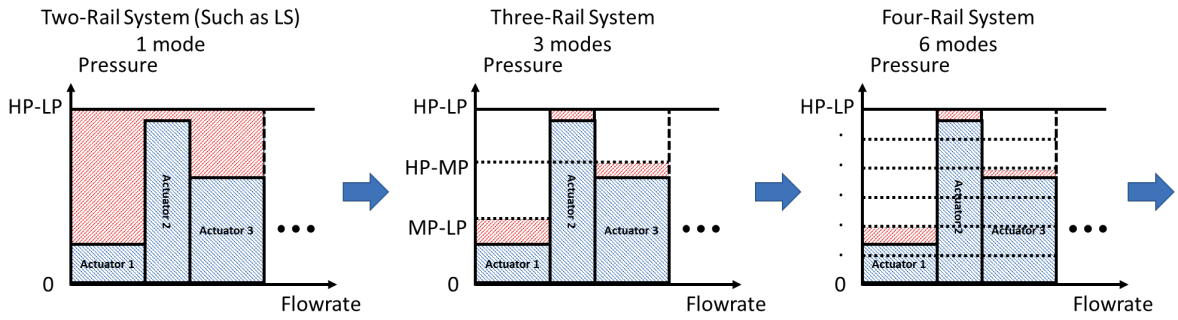

Figure 3: Number of Modes w.r.t Number of Rails and Its Throttling Loss.

The optimal number of rails results in a compromise between cost and energy savings, depending on the particular application. As the representative of an application with numerous functions under resistive loads suitable for MPR implementation, the authors considered the case of an agricultural planter. By considering typical working cycles for a planter, **Table 1** summarized three operating conditions for four selected high-power actuators in the planter.

Operation Condition	Actuator 1		Actuator 2		Actuator 3		Actuator 4	
	$\frac{q_1}{q_{rated}}$	$\frac{p_1}{p_{rated}}$	$\frac{q_2}{q_{rated}}$	$\frac{p_2}{p_{rated}}$	$\frac{q_3}{q_{rated}}$	$\frac{p_3}{p_{rated}}$	$\frac{q_4}{q_{rated}}$	$\frac{p_4}{p_{rated}}$
Normal	55.1	12.5	62.0	22.8	67.4	38.9	21.4	21.3
Fast	72.6	12.7	81.4	37.1	75.1	49.9	25.7	33.2
Max.	90.0	15.1	99.4	54.6	83.7	67.5	30.0	45

Table 1: Normalized Speed and Load Pressure for the Four Motors in a Planter for Different Working Cycles.

Random combinations of the operating conditions for all actuators are made (a total of 81 cases) for system power loss analysis. For such analysis, the pressure drop at the control valve for each actuator in each case needs to be estimated first. The pressure drop depends on which mode the actuator operates. The total pressure range is evenly divided by the number of modes for each rail design. The pressure that divides two different modes is called mode-shifting pressure (MSP). A pressure margin is added to the actuator load pressure to ensure adequate control of the related function. The sum of the load pressure and the pressure margin is compared to the MSPs to determine which mode the actuator is in. Take the three-rail system as an example, if the actuator pressure is higher than the MSP $p_{MP} - p_{LP}$, but lower than the MSP $p_{HP} - p_{LP}$, then this actuator will operate in mode HP-LP. When the modes for each actuator are selected, Equation (3) is used to calculate the power loss:

$$P_{PL} = \sum_{i=1}^{\#\ of\ Actuator} \left(p_{in_i} - \Delta p_i - p_{out_i}\right) \cdot q_i \tag{3}$$

Then, the calculation above is run for all possible working combinations of the actuator. For the total of 81 cases, the calculation results are shown in **Figure 4**. The left plot shows the percentage of loss power reduction for all 81 cases comparing the two-rail system to a system with a variable number of rails. The right plot shows the average of all the cases for each number of rails. It can be seen that the largest loss reduction occurs when increasing the number of rails from 2 to 3. Although the trend is clear, the plot shows scenarios where an increased number of rails reduces the power savings. This is a side effect of the assumption that the additional modes created by adding pressure levels are evenly distributed, rather than adjusting for the optimal values. This assumption greatly speeds up the calculations performend in this analysis. The effect is minor, and taking the average across all cases allows the results to be accurately interpreted.

It is reasonable to state here that the three-rail system is the best choice considering the power loss reduction, the system cost and the added complexity to the system. As a result, the supply system and the pressure select and control valve set in this research work are designed for a three-rail system setup.

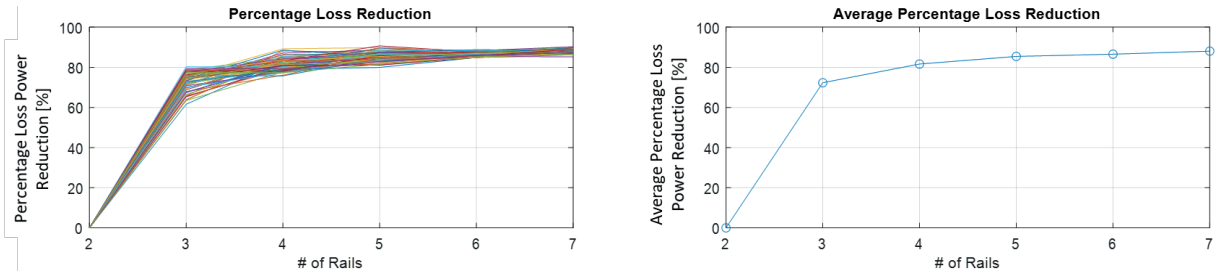

Figure 4: Throttling Loss Reduction w.r.t Number of Rails (Left: Reduction in %, Right: Average Reduction).

2.2 Supply System Design

The supply system is powered by a prime mover, such as an engine, to supply flow to the rails and control their pressure. The selected three-rail system includes a high-pressure rail, a medium-pressure rail, and a low-pressure rail. The high and median pressure rails are powered by the supply unit. The low-pressure level is directly connected to an open tank.

Two architectures can be adopted to achieve the control of a three-rail system for the investigated application. The two options are illustrated in **Figure 5**. Option 1 includes one pump (p_1), one switching valve (V_{SW}), and two accumulators (Acc_{HP}, Acc_{MP}). This design uses a single pump to supply both rails by switching the pump connection between the two pressure rails. Accumulators are used to store pressurized flow. During operation, the pump connects to one rail and provides the total flow for the actuators that are powered by that rail plus some additional flow. This additional flow is used to charge the accumulator and, when the pump is switched to the other rail, the stored pressurized fluid in the accumulator is released to power the actuators.

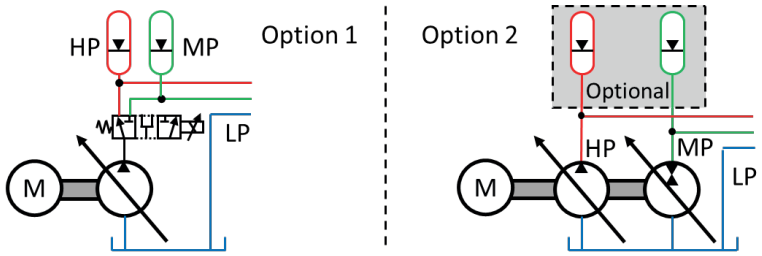

Figure 5: Supply System Design Options.

Option 2 includes two pumps (p_{HP}, p_{MP}), and two optional accumulators (Acc_{HP}, Acc_{MP}). One pump is dedicated to supply flow to each rail. The accumulator is only optional and it should be adopted only if the pumps cannot handle the pressure variations in the rails. The medium-pressure rail pump needs to be an over-center pump. The reason is that there are possible instances where several actuators are in mode 2 and send more flow back into the medium-pressure rail than the actuators working in mode 1 need. In this situation, there is an excess of flow in the medium-pressure rail that needs to go somewhere. If the medium-pressure rail pump does not have the over-center functionality, the excess flow needs to burn through a pressure relief valve, which results in an extremely inefficient solution. With an over-center pump, the unit can work as a motor and handle the excess flow while transferring the power back to the engine shaft.

The pump sizing for option 1 is straightforward. The pump size needs to be large enough to supply the maximum flow required by the system. Option 2 uses two pumps, meaning the individual units can be smaller, with the constraint that their combined flow exceed the maximum required flow command. Based on the representative working condition of the target application, the two pump sizes could be optimized based on overall system efficiency. A parallel working mode is necessary for the option 2 with two smaller units. During worst case scenario, the flow from both pumps could merge with the two pumps operating as a larger unit to fullfill the maximum flow request.

2.3 Pressure Select and Control Valve Set Design

The pressure select and control valve set is the key part for the actuator control in the MPR system. It includes two functionalities: direct the fluid from the rails to the actuator using the on/off valves based on its operation mode, and control the actuator speed using the proportional valves. The operation mode is decided based on the actuator load pressure and the rail pressures. This study proposes two options as shown in **Figure 6**.

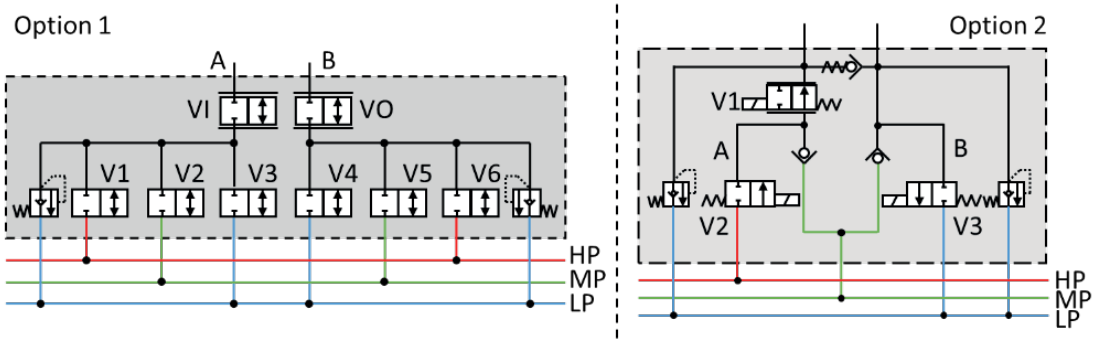

Figure 6: Pressure Select and Control Valve Set Design Options.

Option 1 is the most universal alternative. It contains six on/off valves (V1 to V6) and two proportional valves (VI and VO) that provide all possible connections for the actuator inlet (port A) and outlet (port B). For example, if the actuator is determined to operate in mode 1, V2 and V4 are activated while V1, V3, V5 and V6 remain closed. The opening of either one of VI or VO is adjusted to regulate the flow to the actuator while the other one is fully opened to reduce the throttling loss. **Table 2** shows the on/off valve control strategy under different modes with flow direction from A to B. For agricultural applications, only modes M-L, H-M, and H-L are used (red in the table) and they are named mode 1, 2 and 3 in this study.

	H-H	H-M	H-L	M-H	M-M	M-L	L-H	L-M	L-L
V1	ON	ON	ON	OFF	OFF	OFF	OFF	OFF	OFF
V2	OFF	OFF	OFF	ON	ON	ON	OFF	OFF	OFF
V3	OFF	OFF	OFF	OFF	OFF	OFF	ON	ON	ON
V4	OFF	OFF	ON	OFF	OFF	ON	OFF	OFF	ON
V5	OFF	ON	OFF	OFF	ON	OFF	OFF	ON	OFF
V6	ON	OFF	OFF	ON	OFF	OFF	ON	OFF	OFF

Table 2: Valve Control Strategy for Pressure Select and Control Valve Set Design Option 1.

Option 2 is a simplification from option 1 by considering the typical operating conditions for agricultural applications (section 2.1). Port B never needs to connect to the high-pressure rail therefore no metering control valve is needed for port B. As a result, only one proportional valve (V1) and two on/off valves (V2 and V3) are required for option 2. Option 2 cannot achieve all the modes the first variant can, but it is sufficient for agricultural applications. **Table 3** shows the valve control strategy under different modes with flow direction from A to B.

	H-H	H-M	H-L	M-H	M-M	M-L	L-H	L-M	L-L
V1	N/A	Active	Active	N/A	Active	Active	N/A	Off	Off
V2		On	On		Off	Off		Off	Off
V3		Off	On		Off	On		Off	On

Table 3: Valve Control Strategy for Pressure Select and Control Valve Set Design Option 2.

3 Controller Design

The controller for the proposed MPR system has several components. It includes a supervisory controller, a pump controller, and the actuator controller. **Figure 7** shows the control flow chart of the proposed MPR system.

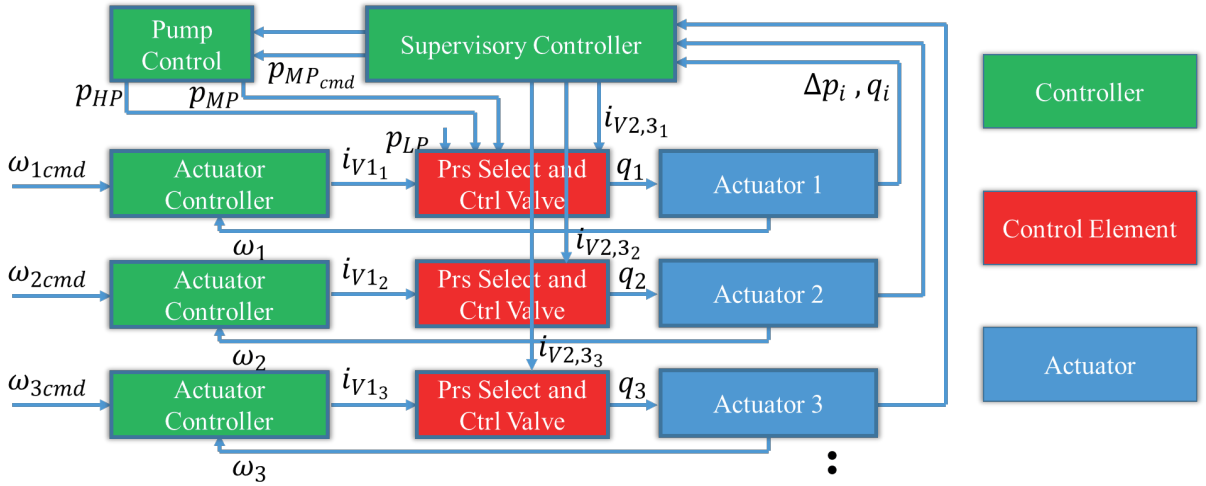

Figure 7: MPR System Controller Overview Block Diagram.

The actuator controller adjusts the metering valve tracking the actuator performance through speed feedback. The actuator load pressure and flow rate are fed into the supervisory controller. The supervisory controller selects the necessary pressure for each rail and the operating mode for each actuator. The operating mode command is executed by the pressure select and control valve set, and the desired rail pressure is sent to the pump controller. Finally, the pump controller regulates the supplying pumps to reach and maintain the desired rail pressure.

3.1 Actuator Controller

As the operating mode is determined by the supervisory controller, the actuator controller only regulates the opening of the proportional metering valve(s). For this research, this controller is a PI controller with an anti-

windup that performs a speed control loop with the error between commanded and measured speed as input. The output of the speed controller is the actual valve opening command to the metering valve.

3.2 Supervisory Controller

The supervisory controller has two missions to accomplish. The first task is to determine the operating mode for each actuator. The second task is to determine the best rail pressures that minimize the throttling loss in the system. An optimization algorithm is adopted in this study to find the best high-pressure and median-pressure levels with the corresponding actuator operating mode combination.

The high-pressure rail pressure p_H is determined using Equation (4). Δp_i is the actuator load pressure and p_{mar} is the pressure margin that ensures the control valve has sufficient pressure drop to operate.

$$p_H = \max(\Delta p_1, \Delta p_2, \dots, \Delta p_n) + p_{mar} \tag{4}$$

The total power loss in the system is defined as in Equation (5). P_{PL} is the total power loss in the system, i represents the related actuator, p_{in_i} is the inlet pressure for i_{th} actuator before the control valve, p_{out_i} is outlet pressure of the i_{th} actuator, Δp_i and q_i are the load pressure and flowrate for the i_{th} actuator, $p_{H/M/L}$ are the pressure in the three rails. q_{ex} is the surplus flow in median-pressure rail, and η_{MP_V} is the volumetric efficiency of the median-pressure rail pump when it is acting as a motor. The first part of Equation (5) includes all the throttling loss from the control valves, and the second part corresponds to the power loss for any surplus flow in the median-pressure rail that goes through the over-center pump.

$$P_{PL} = \sum_{i=1}^{n} (p_{in_i} - \Delta p_i - p_{out_i}) q_i + (p_M - p_L)(1 - \eta_{MP_V}) q_{ex} \tag{5}$$

The challenge here is that the function is discontinuous as p_{in/out_i} depends on the mode the actuator operates in. For a three-rail-three-actuator MPR system, there are 27 possible actuator-mode combinations, which are called cases in this study.

Fortunately, some of the cases can be excluded from the calculation of the total power. First, the actuators are sorted in descending order of their load pressure (Aa, Ab and Ac). This means Aa should always be in mode 3 as it is the highest load pressure among all actuators. This leaves only nine cases left. Among these nine cases, five of them always result in higher power consumption when compared to the other four. For example, the case with operating mode 3-2-2 for actuators Aa to Ac is always worse than the case 3-1-1. The reason is that the first case requires the medium-pressure pump to take the flow from all the actuators while working as a motor. This configuration introduces more losses than the other case because of the pump efficiency. Similar conclusions can be drawn from the comparison of the other cases.

The corresponding power loss equation for the four remaining cases is listed in **Table 4**.

Case	Actuators			Power Loss
	a	b	c	
1	3	1	1	$P_{PL_1} = [(p_H - p_L) - \Delta p_a] q_a + [(p_M - p_L) - \Delta p_b] q_b + [(p_M - p_L) - \Delta p_c] q_c$
2	3	1	2	$P_{PL_2} = [(p_H - p_L) - \Delta p_a] q_a + [(p_M - p_L) - \Delta p_b] q_b + [(p_H - p_M) - \Delta p_c] q_c + (p_M - p_L) \max(q_c - q_b, 0)(1 - \eta_{MP_V})$
3	3	2	1	$P_{PL_3} = [(p_H - p_L) - \Delta p_a] q_a + [(p_M - p_L) - \Delta p_b] q_b + [(p_M - p_L) - \Delta p_c] q_c + (p_M - p_L) \max(q_b - q_c, 0)(1 - \eta_{MP_V})$
4	3	3	1	$P_{PL_4} = [(p_H - p_L) - \Delta p_a] q_a + [(p_H - p_L) - \Delta p_b] q_b + [(p_M - p_L) - \Delta p_c] q_c$

Table 4: Power Loss Calculation for All Cases.

By rearranging the equations and cancelling out the common terms in all cases, **Table 5** shows the final power loss equation for the four cases. The same table in the right column shows the constraints for each case. These constraints restrict the available pressure levels for the medium pressure rail. For example, in Case 1, the constraint is that the medium pressure be higher than the load pressure of actuator 1 and 2, plus the pressure margin (p_{mar}). In Case 2, however, because mode 2, connecting HP to MP is included, the medium pressure must also be low enough that the pressure drop from HP to MP exceeds the load on the mode 2 actuator plus the pressure margin. If these constraints cannot be met in the selected case, the case is excluded from the rest of the calculation. The objective here is to find the value of p_M within the constrains for each case that minimizes the power loss. The partial equation in red for each case is not relevant to p_M and can be treat as constants. Then, the equation becomes a simple linear r be select and vise versa. Finally, the lowest possible power loss out of the four cases will be chosen as the control strategy.

Case	Actuators			Power Loss	Constrains
	a	b	c		
1	3	1	1	$P_{PL_1} = p_M(q_b + q_c) + p_H(q_a) - p_L(q_a + q_b + q_c)$	$(p_M - p_L) - \Delta p_b > p_{mar}$
2	3	1	2	$P_{PL_2} = p_M(q_b - q_c) + p_H(q_a + q_c) - p_L(q_b + q_a) + (p_M - p_L)\,max(q_c - q_b, 0)\,(1 - \eta_{MP_V})$	$(p_M - p_L) - \Delta p_b > p_{mar}$ $(p_H - p_M) - \Delta p_c > p_{mar}$
3	3	2	1	$P_{PL_3} = p_M(q_c - q_b) + p_H(q_a + q_b) - p_L(q_a + q_c) + (p_M - p_L)\,max(q_b - q_c, 0)\,(1 - \eta_{MP_V})$	$(p_H - p_M) - \Delta p_b > p_{mar}$ $(p_M - p_L) - \Delta p_c > p_{mar}$
4	3	3	1	$P_{PL_4} = p_M(q_c) + p_H(q_a + q_b) - p_L(q_a + q_b + q_c)$	$(p_M - p_L) - \Delta p_c > p_{mar}$

Table 5: Final Power Loss Equation for the Four Cases and Their Constraints.

If the power loss difference between each case is small, a minor disturbance can change the selected case. This can result in excessive case switching, which is not ideal because it will make the system less stable. A simple switching resistance strategy can be achieved by setting a loss margin P_{mar}. If the power loss in the current time step is not better than the last time step plus this margin, the algorithm does not command to switch the operating case. This strategy imposes a small sacrifice on the power loss reduction to prevent excessive case switching. During transient stage, the system pressure and flow varies very fast. As a result, the power varies largely during the transient period, and the loss margin is unable to prevent excessive switching. To prevent excessive case switching specifically during the transient period, a debouncing time margin (t_{mar}) is added that prevents the system case from switching until the the specified time between switches has elapsed, or there is a command change.

3.3 Pump Controller

The control strategy developed for the supply system varies depending on the selected variant of the supply system, single pump (Option 1) or multiple pumps (Option 2). Both strategies make use of the reference pressure command provided by the supervisory controller in addition to a pressure feedback controller. The pump controller eventually acts on the pump(s) displacement and regulates the opening of the switching valve V_{SW} to regulate the pressure in each rail.

3.3.1 Single Pump Controller

Figure 8 shows the structure of the controller adopted for a supply unit composed of a single pump, a switching valve and one accumulator for each rail. This variant of the supply unit is labelled as Option 1 in this document. p^*_h and p^*_m refer to the high and medium pressure setpoints respectively selected by the supervisory controller, while p_h and p_m refer to the measured high and medium pressure rail pressure levels.

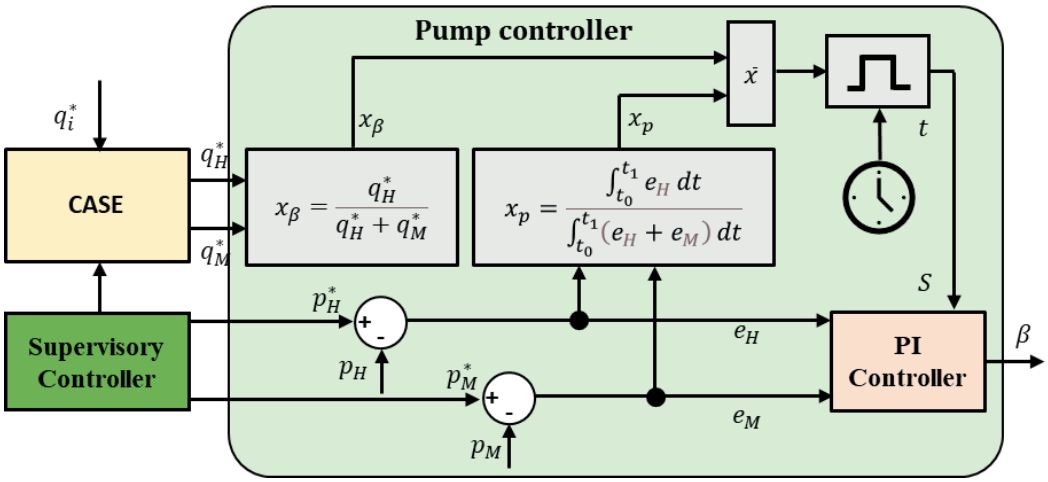

Figure 8: Single Pump Controller Block Diagram.

The duty cycle S of the switching valve is regulated based on the calculated error of the commanded pressure levels (e_h, e_m.) averaged with the ratio of flow commands between the medium and high pressure rails. The integral of the error between commanded and measured pressure e_{p_i} over a specific period of time t is used rather than the error itself. Because of the constant oscillation of the pressure in the rails, the accumulated error provides a better estimate of the error over the analysed period of time. A ratio x_p is defined as in Equation (6). An x_β term is also generated as shown in Equation (7). This term acts similarly to a feed forward term. These terms are averaged to get $\bar{x}$. This term corresponds to the percentage of the defined period the supplying pump spends connected to each rail. The ratio ranges from 0 to 1, which means that the pump is providing flow to only the MP rail, if $\bar{x} = 0$, or to only the HP rail if $\bar{x} = 1$

$$x_p = \frac{\int_{t_0}^{t_1} e_H\, dt}{\int_{t_0}^{t_1}(e_H + e_M)\, dt} \tag{6}$$

$$x_\beta = \frac{q_H^*}{q_H^* + q_M^*} \tag{7}$$

The duty cycle S corresponds to a square command with a ratio equal to $\bar{x}$ and period t as in Equation (8).

$$S = square(t, \bar{x}\,) \tag{8}$$

If $S = 1$ the pump delivers flow to the HP rail while if $S = 0$ the flow is directed to the MP rail.
The feedback controller is a traditional Proportional-Integrative (PI) controller with an anti-windup strategy whose parameters were manually tuned based on the pump response to the given commands. Equation (9) summarizes the feedback terms $\beta_{FB,H}$ and $\beta_{FB,M}$ in function of the calculated error.

$$\beta = \begin{cases} \beta_{FB,H} = k_P e_H + k_I \int e_H\, dt & if\ S = 1 \\ \beta_{FB,M} = k_P e_M + k_I \int e_M\, dt & if\ S = 0 \end{cases} \tag{9}$$

3.3.2 Multi-Pump Controller

The multi-pump controller is also based on a pressure feedback strategy with a flow feedforward term. In this case, both pumps are controlled entirely independently. The overall structure of the controller is outlined in **Figure 9**.

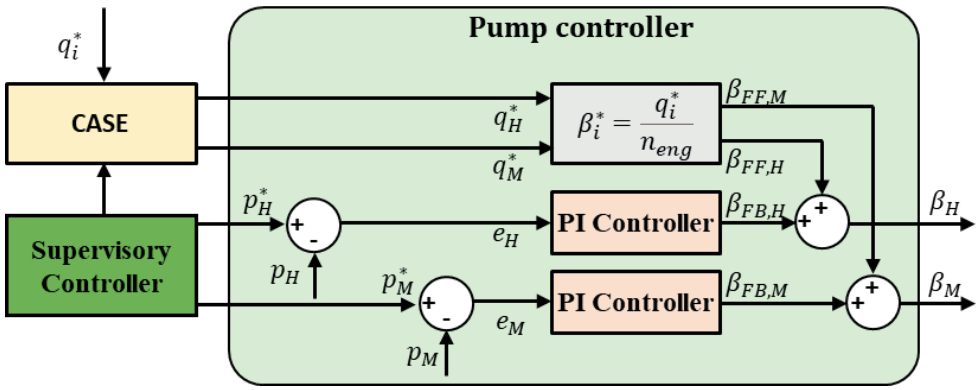

Figure 9: Multi-Pump Controller Block Diagram.

4 Test-rig Design and Simulation Model

Due to the multiple supply configurations being considered, the architecture selected for the test rig was designed with the goal of being switchable between the two configurations. A significant portion of its hydraulic architecture is shown in **Figure 10**. The core of this flexibility is found in the supply system, which can operate in three modes. The first configuration uses both pumps (item 2) to represent supply option 2 with optional accumulators (item 5). This is the default configuration of the system. The second configuration uses only the pumps, with the accumulators isolated by shutting off the valves at the ports, which also represents supply option 2 but without accumulators. The final configuration uses only one pump, switched between the high and medium pressure rails using the switching valve (item 3), which represents supply option 1, with the pressure level stabilized by the accumulators and the unused pump set to zero displacement and routed to tank through the unloading valve (item 4).

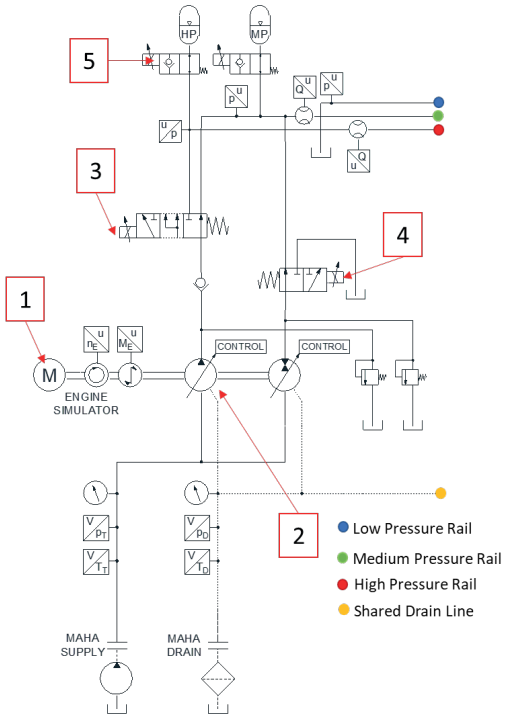

Figure 10: Supply Section of MPR Test Rig

The required flow for any specific work cycle does not affect the sizing of the accumulators because the accumulators will eventually run dry for typical long actuation periods of the motoring functions, regardless of the volume of the hydraulic capacitance. For this reason, the maximum allowed pressure variation for a specific working condition is the only determining factor in the sizing of the accumulators. In this study, the known Equation (10) is used to calculate the size of the accumulators [1].

$$V = \frac{\left(\frac{p_2}{p_1}\right)^{\frac{1}{\gamma}} \Delta V}{\left(\frac{p_0}{p_1}\right)^{\frac{1}{\gamma}} \left[\left(\frac{p_2}{p_1}\right)^{\frac{1}{\gamma}} - 1\right]} \tag{10}$$

Where V corresponds to the calculated volume. p_1 and p_2 are the minimum and maximum pressure of the allowed oscillation range. ΔV is the difference in gas volume from p_1 to p_2. p_0 is the gas pre-charge value of the accumulator and γ corresponds to the polytropic exponent.

The implement control valve was implemented with the schematic that is shown in **Figure 11**, for one actuator. The schematic shown in this figure is repeated for the other two actuator and control valve assemblies, attached to the high, medium, and low-pressure rails as shown.

To simulate the load on the system, a compact load unit is used, consisting of a gear motor connected directly via an internal shaft to a gear pump. The gear pump is loaded through an electronically controlled proportional relief valve.

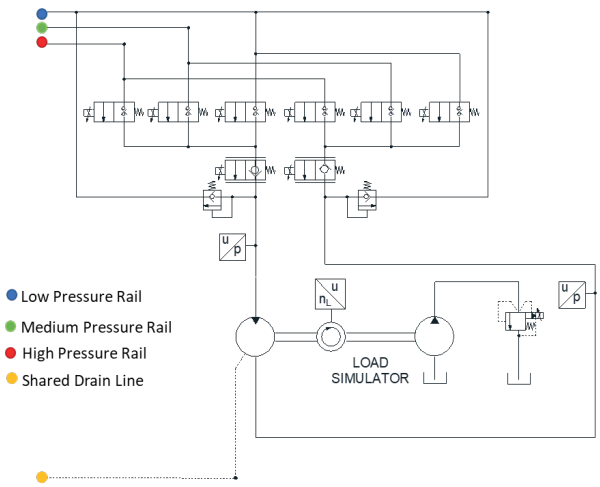

Figure 11: MPR Test Rig Load Unit and Control Valve Assembly

The architecture outlined above was implemented on a test stand at Maha Fluid Power Research Labs, using components provided by Bosch Rexroth, and with component selection assistance from them. In addition to the hydraulic components, Bosch Rexroth also supplied the BODAS software for the pump controller that automatically regulates the actual displacement angle, following the given command. Control and data acquisition was done using a National Instruments CRio 9024, outfitted with the necessary IO cards. The controller was implemented using Simulink and was connected to the CRio using NI Veristand. **Figure 12** shows images of the completed test rig, and **Table 6** provides information on the hydraulic components.

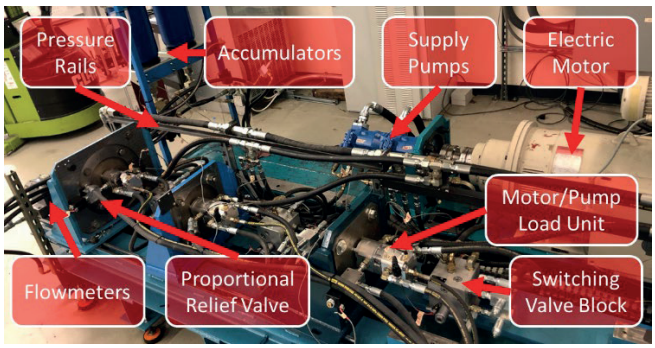

Figure 12: Physical Implementation of Hydraulic Circuit

Component	Quantity	Manufacturer	Model Number	Specifications
Axial Piston Pump	2	Bosch Rexroth	R902578344	45 cc/rev
Switching/Unloading Valve	2		R933001723	2 – 140 lpm
High Pressure Accumulator	1		R901435307	32 L
Medium Pressure Accumulator	1		R901435305	20 L
Accumulator Shutoff Valve	2		R930067154	2-way on/off
Implement Control Valve	3		Custom Assembly	0 – 70 lpm
Load Unit	3		R979PT1067	8 cc gear motor 8 cc gear pump
El. ctrl. Pressure Relief Valve	3		R934001537	20 – 220 lpm 8 – 150 lpm
BODAS Pump Controller	2		-	CAN J1939 Protocol

Table 6: Hydraulic Components Used in Construction of Test Stand

5 Simulation and Measurement Result

The target of the test setup is to investigate the controllability, tracking performance, and energy consumption of the MPR architecture with several motoring functions. The MPR system was first simulated by providing the values of pressure and flow of each actuator to the supervisory controller. The supervisory controller provides the optimal modes and related estimation of the power consumption for the different working conditions. Such power consumption calculation also takes into account fixed restrictions, fittings and length of the lines on the actual stand alone test rig. An additional pressure drop is therefore calculated as a function of the flow across each hydraulic line and added to the defined pressure margin p_{mar}. The simulated system is advantageous as it provides guidelines to identify the mode switching points and can be used to estimate the hydraulic power consumption for several working conditions.

Figure 13 shows the mode selection strategy for a specific range of working conditions taken as reference. The range of working conditions shown in the maps consider the case where actuator 1, has the highest load, held constant ($p_1 = 150\ bar$ and $q_1 = 10\ lpm$). The other two functions (2 and 3) vary in pressure, from 5 to 150 bar, and are considered for two different flow rates. In Figure 13 q_2 corresponds to 5 lpm (left maps), and 10 lpm (right maps). q_3 is equal to 5 lpm in the top maps and to 10 lpm in the bottom ones.

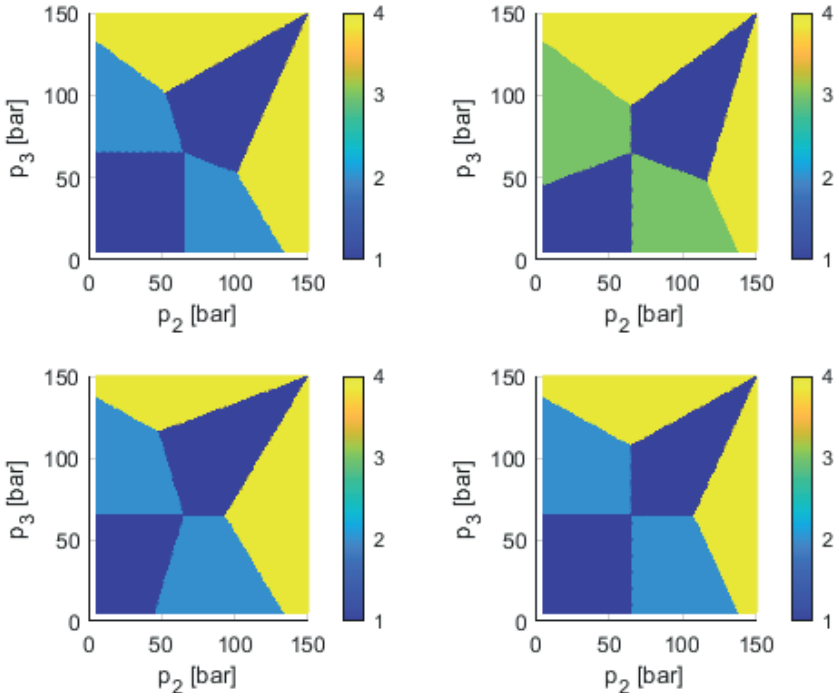

Figure 13: Mode map for varying operating conditions.

In Figure 13, the modes that are selected define the case for each operating point. The mode configurations corresponding to each of the cases above are shown in **Table 7**.

Case \ Actuator	1	2	3
	Mode		
1	3	1	1
2	3	3	1
	3	1	3
3	3	2	1
4	3	1	2

Table 7: CASE options in reference to Figure 13.

A conceptual LS system is adopted for comparison on the estimation of hydraulic power consumption P_{hyd}. The power consumption corresponds to the power provided by the hydraulic supply units and is calculated as stated in

Equation (11) based on the pumps outlet flow $q_{P,HP}$ and $q_{P,MP}$ and pressures p_{HP} and p_{MP}. The power calculations for the LS system are instead estimated by summing the overall flow delivered by the supply unit while the high-pressure rail is considered.

$$P_{hyd} = \begin{matrix} q_{P,HP} * p_{HP} + q_{P,MP} * p_{MP} & MPR \\ \left(q_{P,HP} + q_{P,MP}\right) * p_{HP} & LS \end{matrix} \tag{11}$$

The model above was used to simulate the performance of the system across a range of operating conditions. **Figure 14** shows a power consumption mesh generated for a fixed load on actuator 1, and varied loads for actuators 2 and 3. Similar meshes were generated for a variety of loads on actuator 1. This simulation was then validated by taking steady state measurements at a variety of points around the map. These are indicated by the red circles. As can be seen, the experimental and simulated power consumption values track quite closely with one another, meaning the simulation is valid for estimating power consumption values.

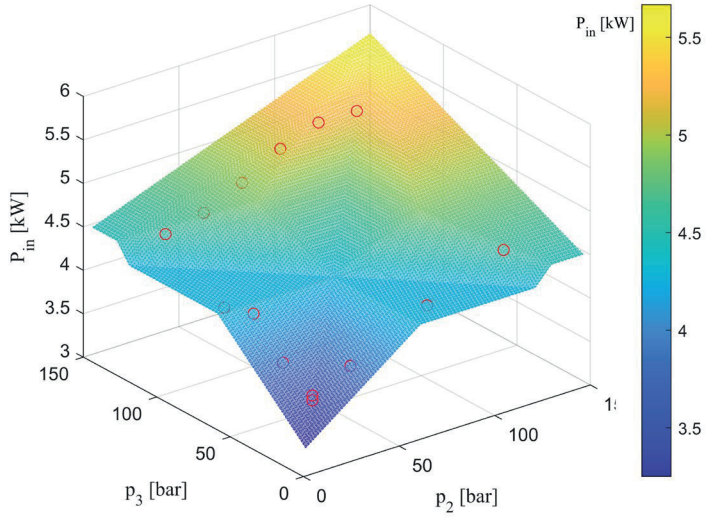

Figure 14: MPR Experimental Validation of the Hydraulic Power Consumption Map.

After validating the simulation, it was compared against a theoretical load sensing system, modeled as shown previously in Equation (5), and the improvement in efficiency was calculated. **Figure 15** below shows the resulting surface for the same configuration as the power consumption validation map. The map shows that the highest improvement in efficiency occurs at low load conditions for actuators 2 and 3. This makes sense, as this is the most inefficient condition for a conventional load sensing system to run in. Conversely, savings are lowest at high loads, where the MPR system functions similarly to a conventional load sensing system, and where throttling losses are the smallest. As before, these calculations were performed for several load settings for actuator 1. Averaging across all the cases led to an average efficiency gain of 45%.

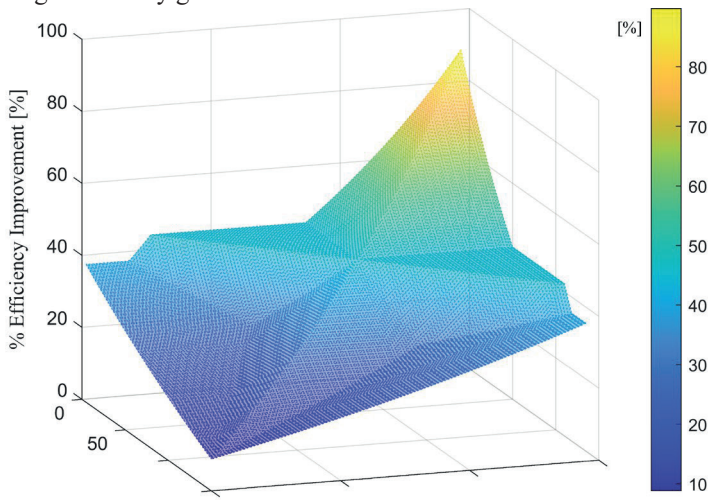

Figure 15: Simulated Efficiency Gain of MPR System Over Theoretical Load Sensing System.

In addition to power consumption, it was neccessary to validate the controllability and stability of the system. To this end, a test drive cycle was developed. The drive cycle is divided into four sections, from (A) to (D) as shown for the one pump configuration in **Table 9**. The first switch, from operating condition A to B simply involves increasing a single load unit commanded load while holding the commanded speed constant. The medium pressure rail rises to meet the demand of this user, while the speed holds constant. The first step induces the variation of mode of only one actuator. Another simple load increase from section (B) to (C) results in the mode switch of two actuators. The third step is even more complex as all three actuators switch modes at once. For the two pump system, modified drive cycle had to be devised, as shown in **Table 9**. This is because, while the two pump system could run the one pump drive cycle without issue, its lower pressure margin meant that the system did not need to perform all mode switches to be in the optimal operating condition. This was resolved by lowering several of the load pressures slightly, and resulted in both tests performing the same switches.

Time	(A) 0-10s		(B) 10-50s		(C) 50-90s		(D) 90-130s	
	Command	Mode	Command	Mode	Command	Mode	Command	Mode
$\omega_{1_{cmd}}\,[rpm]$	1200	3	1200	3	1200	3	600	2
$p_{1_L}\,[bar]$	160		160		160		40	
$\omega_{2_{cmd}}\,[rpm]$	800	1	800	1	800	3	800	1
$p_{2_L}\,[bar]$	40		80		140		80	
$\omega_{3_{cmd}}\,[rpm]$	600	1	600	2	600	1	1200	3
$p_{3_L}\,[bar]$	40		40		40		160	

Table 8: Test Drive Cycle for One Pump Configuration.

Time	(A) 0-10s		(B) 10-30s		(C) 30-50s		(D) 50-70s	
	Command	Mode	Command	Mode	Command	Mode	Command	Mode
$\omega_{1_{cmd}}\,[rpm]$	1200	3	1200	3	1200	3	600	2
$p_{1_L}\,[bar]$	160		160		160		20	
$\omega_{2_{cmd}}\,[rpm]$	800	1	800	1	800	3	800	1
$p_{2_L}\,[bar]$	20		100		140		100	
$\omega_{3_{cmd}}\,[rpm]$	600	1	600	2	600	1	1200	3
$p_{3_L}\,[bar]$	20		20		20		160	

Table 9: Test Drive Cycle for Two Pump Configuration

The one pump configuration test results are shown in **Figure 16**. The plot on the top shows the speed tracking of the three actuators, the central plot shows the actuator load tracking, and the bottom plot shows the mode for each actuator.

For the first two simple shifts, as the actuator 2 command load incrases, the mode switcing is clean. For the third, complex switch, a debounce logic prevents chattering by performing the switch in two stable steps. The steady state behaviour of the one pump system is acceptable, although oscillations due to the constant switching of the pump between rails are visible. The accumulators serve to stabilize this somewhat, but in high flow command situations, such as for actuators 1 and 2, they cannot entirely dampen the effects of the pump switching. They also come at the cost of slow load tracking rise times, as seen at 50 and 90 seconds, where the accumulators must charge before reaching full torque across the motors. In spite of this, however, the system behaves stabily and predictable, and the switches, including the complex one at 100 seconds are performed reasonably cleanly.

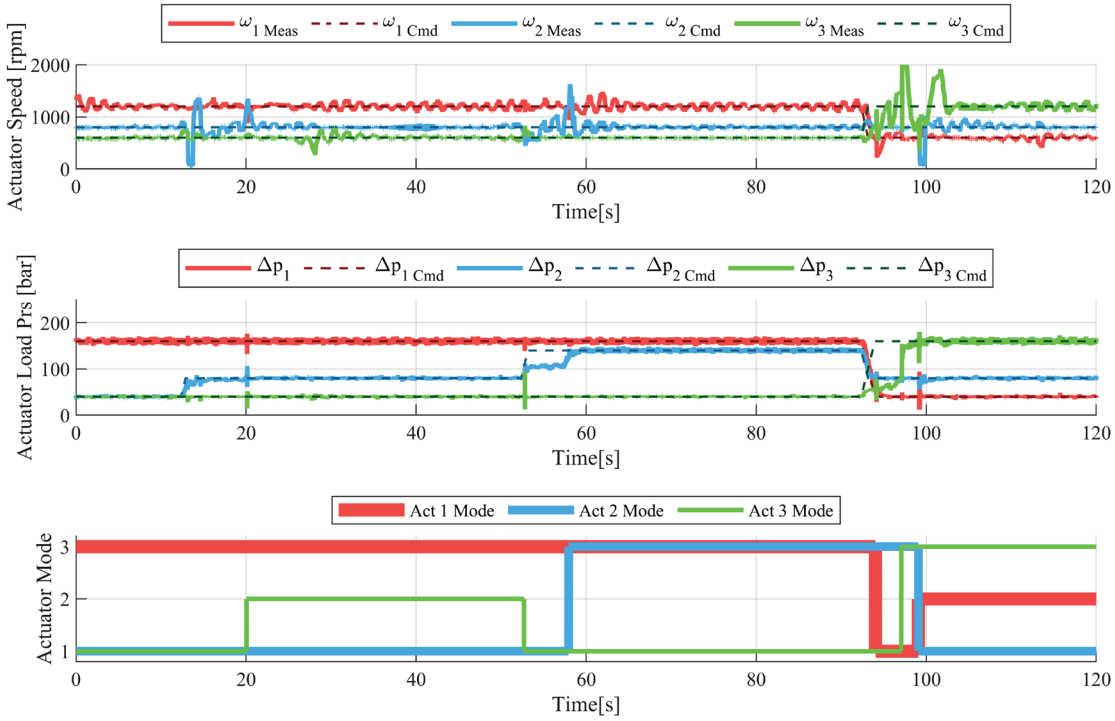

Figure 16: Drive Cycle Tracking Results – One Pump Configuration

Figure 17 below shows the results of the two pump test. It is clear that the performance, both steady state and dynamic of the two pump configuration is far cleaner and less prone to instability. Transient oscillations settle out quickly and steady state tracking is nearly perfect. The switching logic also prevents chattering and instability in complex switches such as the one occurring at 55 seconds. This set of results demonstrates well the effectiveness of the architecture and control strategy previously outlined.

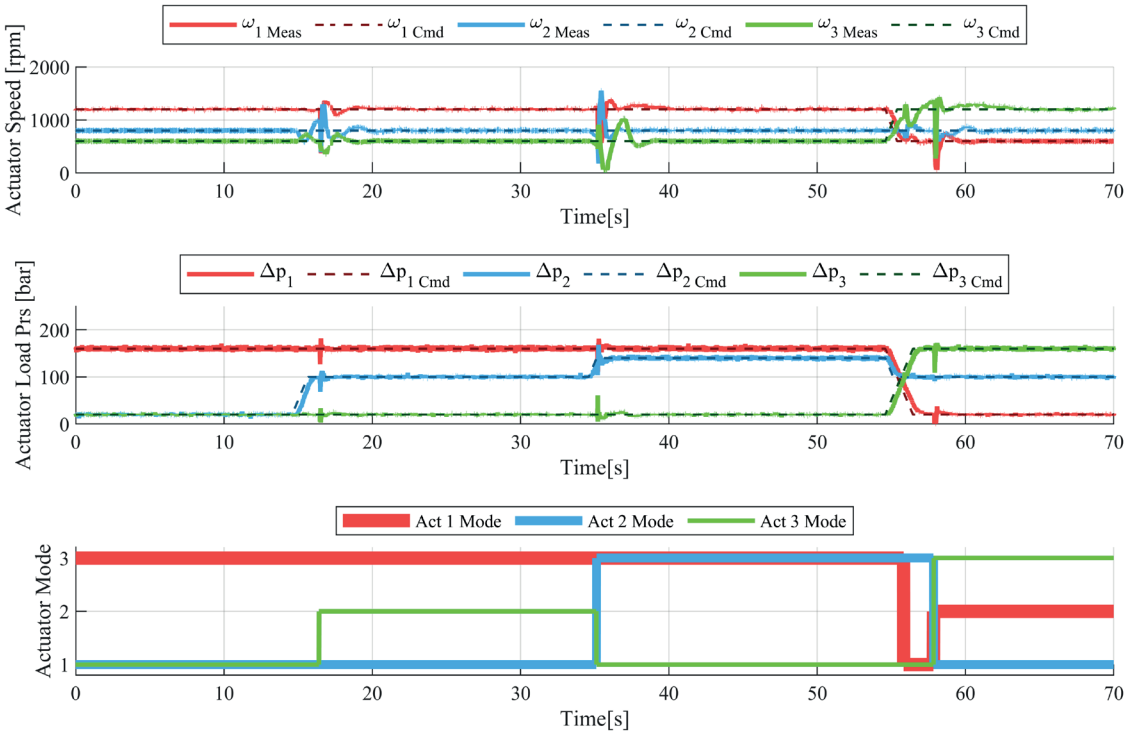

Figure 17: Drive Cycle Tracking Results – One Pump Configuration

6 Conclusion

This paper presents the design of a Multi-Pressure Rail (MPR) system suitable to power multiple hydraulic functions with a centralized supply system. The target of the system is to minimize throttling losses and be applicable in systems with a large number of functions with no significant opportunity for energy recuperation. Such system could effectively replace the conventional load sensing systems that are used to power hydraulic remotes in off-road vehicles, such as in agricultural tractors.

The paper discusses a design based on three pressure rails, representing the optimal compromise for systems such as agricultural tractors and implements such as planters. Different alternatives for implementing the MPR system are presented, including different layouts to control the rails: one layout is based on two pumps, each one dedicated to a single pressure rail, and the other layout utilizes a single pump connected to two accumulators. A controller that manages the pressure in the rail based on the load pressure (supervisory controller) is discussed, along with a controller designed to select the rail configuration and control the valve set connected to each actuator. The specific design of these valve sets is discussed.

A stationary test rig is developed at the Maha Fluid Power Research Center of Purdue University to demonstrate the performance of the MPR solution and its controller with actual components. The paper illustrates the test design and results in both steady state and transient operation.

For the steady state results, the modes of operation of the system are illustrated. For the sake of showing the energy efficiency potentials, these results are compared a theoretical traditional load sensing system for the same working conditions. These results show an average efficiency improvement across all operating conditions of 45%.

The transient results are shown to assess the validity of the formulation of the controller. These results show the ability of the MPR system to properly modify its configuration to follow the commands and the load variation while maximizing efficiency. Overall, the simulation and experimental results show success in the system's goals of reducing throttling losses by varying the pressure setting of the medium pressure rail.

Acknowlagement

The project is funded by the Department of Energy, USA (DOE project DE-EE0009201, 'A New Approach for Increasing Efficiency of Agricultural Tractors and Implements').

Nomenclature

$\#mode$	Number of modes
$\#rail$	Number of rails
P	Power
p	Pressure
Δp	Pressure difference between the inlet and outlet of the actuator
q	Flowrate
β	Hydraulic Unit Displacement
η	Efficiency
V	Switching Valve
ω	Rotational speed
x	Time ratio
S	Duty cycle
V	Volume of the Control Volume
t	Time
p^*	Commanded Pressure
γ	Isotropic Expansion Constant
k	Constant, usually application tuned
e	Error from a measured value to a setpoint
Subscripts	
mar	Margin

cmd	Command
H/HP	High pressure rail
M/MP	Median pressure rail
L/LP	Low pressure rail
PL	Power Loss
in	Actuator inlet
out	Actuator outlet
i	Actuator
FF	FeedForward control
FB	Feedback control

Reference

[1] A. Vacca and G. Franzoni, Hydraulic Fluid Power: Fundamentals, Applications, and Circuit Design, Wiley, 2021.

[2] L. J. Love, E. Lanke and P. Alles, "Estimating the impact (energy, emissions and economics) of the US fluid power industry," Oak Ridge National Laboratory, Oak Ridge, TN, 2012.

[3] X. Tian, J. C. Gomez, A. Vacca, S. Fiorati and F. Pintore, "Analysis of Power Distribution in the Hydraulic Remote System of Agricultural Tractors Through Modelling and Simulations," in *ASME/BATH 2019 Symposium on Fluid Power and Motion Control*, Longboat Key, Florida, USA, October 7-9, 2019.

[4] X. Tian, P. Stump, A. Vacca, S. Fiorati and F. Pintore, "Power-Saving Solutions for Pre-Conpensated Load-Sensing Systems on Mobile Machines," *Transactions of the ASABE,* vol. 64, no. 5, pp. 1435-1448, 2021.

[5] J. Siebert, M. Wydra and M. Geimer, "Efficiency Improved Load Sensing System - Reduction of System Inherent Pressure Losses," *energies,* vol. 10, no. 7, p. 941, 2017.

[6] H. Murrenhoff, S. Sgro and M. Vukovic, "An overview of energy saving architectures for mobile applications," in *Proceedings of the 9th International Fluid Power Conference*, Aachen, Germany, 2014.

[7] E. Busquets, Advanced Control Algorithms for Compact and Highly Efficient Displacement-Controlled Multi-Actuator and Hydraulic Hybrid Systems, West Lafayette, IN: Ph.D. Thesis, Purdue University, 2016.

[8] H. Murrenhoff, Regelung von verstellbaren Verdrängereinheiten am Konstant-Drucknetz, RWTH Aschen, Germany, 1983.

[9] T. Dreher, "The Capability of Hydraulic Constant Pressure System with a Focus on Mobile Machines," in *Proc. of 6th FPNI-PhD Symp.*, West Lafayette, IN, USA, 2010.

[10] H. Nikolaus, "Antriebssystem mit hydrostatischer Kraftübertragung". Germany Patent DE2739968, 1977.

[11] K. Heybroek and M. Sahlman, "A Hydraulic Hybrid Excavator Based on Multi-Chamber Cylinders and Secondary Control - Design and Experimental Validation," *International Journal of Fluid Power,* vol. 19, no. 2, pp. 91-105, 2018.

[12] G. E. Vael, P. A. Achten and Z. Fu, "The innas hydraulic transformer the key to the hydrostatic common pressure rail," *SAE Technical Paper,* Vols. 2000-01-256.1, 2000.

[13] W. Shen, H. Huang, Y. Pang and X. Su, "Review of the Energy Saving Hydraulic System Based on Common Pressure Rail," *IEEE Access,* vol. 5, pp. 655-669, 2017.

[14] J. Lumkes and J. Andruch, "Hydraulic Circuit for Reconfigurable and Efficient Fluid Power Systems," in *The 12th scandinavian international conference on fluid power*, Tampere, Finland, 2011.

[15] P. Dengler, J. Groh and M. Geimer, "Valve control concepts in a constant pressure system with an intermediate pressure line," in *21st International Conference on Hydraulics and Pneumatics*, Ostrava, Czech Republic, 2011.

[16] P. Dengler, M. Geimer, H. Baum, G. Schuster and C. Wessing, "Efficiency improvement of a constant pressure system using an intermediate pressure line," in *8th International Fluid Power Conference*, 2012.

[17] M. Vukovic, R. Leifeld and H. Murrenhoff, "STEAM - a Hydraulic Hybrid Architecture for Excavators," in *10th Int. Fluid Power Conference*, Dresden, Germany, March 2016.

[18] M. Vukovic, R. Leifeld and H. Murrenhoff, "Reducing Fuel Consumption in Hydraulic Excavators - A Comprehensive Analysis," *Energies,* vol. 10, no. 5, p. 687, 2017.

[19] J. Siefert and P. Y. Li, "Optimal Control and Energy-Saving Analysis of Common Pressure Rail Architectures: HHEA & STEAM," in *Proceedings of the BATH/ASME 2020 Symposium on Fluid Power and Motion Control*, Virtual, Online, 2020.

[20] A. Opgenoorth, C. Hass, K. Frischkorn and K. Schmitz, "Hydraulische Mehrdrucksysteme für mobile Arbeitsmaschinen mit elektrischen Antrieben," in *Hybride und energieeffiziente Antriebe für mobile Arbeitsmaschinen : 8. Fachtagung*, Karlsruhe, German, 23. Februar 2021.